Off-body Channel Measurements at 2.4 GHz and 868 MHz in an Indoor Environment

Evangelos Mellios
SPHERE,
University of Bristol,
Merchant Venturers' Building,
Woodland Road, BS8 1UB, Bristol, UK
Evangelos.Mellios@bris.ac.uk

Angelos Goulianos
SPHERE,
University of Bristol,
Merchant Venturers' Building,
Woodland Road, BS8 1UB, Bristol, UK
A.Goulianos@bris.ac.uk

Sema Dumanli
Telecommunications Research Lab,
Toshiba Research Europe Ltd,
32 Queen Square,
BS1 4ND, Bristol, UK.
Sema.Dumanli@toshiba-trel.com

Geoffrey S. Hilton
SPHERE,
University of Bristol,
Merchant Venturers' Building,
Woodland Road, BS8 1UB, Bristol, UK
Geoff.Hilton@bris.ac.uk

Robert. J. Piechocki
SPHERE,
University of Bristol,
Merchant Venturers' Building,
Woodland Road, BS8 1UB, Bristol, UK
R.J.Piechocki@bris.ac.uk

Ian J. Craddock
SPHERE,
University of Bristol,
Merchant Venturers' Building,
Woodland Road, BS8 1UB, Bristol, UK
Ian.Craddock@bris.ac.uk

ABSTRACT

This paper presents an off-body wireless channel measurement campaign at 2.4 GHz and 868 MHz in an indoor laboratory environment. The performance of different 2.4 GHz antennas is evaluated and it is found that chest-mounted directional patch antennas result in an average of 4 dB higher channel gain than horizontally polarised omnidirectional ones. Comparison of propagation at 2.4 GHz and at 868 MHz shows that when omnidirectional on-body antennas are used in both bands, the lower frequency results in an average of 5 dB higher channel gain. However, when directional patches are employed at 2.4 GHz, the advantage of the 868 MHz is only about 1 dB. Finally, a measurement-based channel model suitable for narrowband system-level simulations is presented.

Keywords
WBANs, Off-body channel measurements, 2.4 GHz band, 868 MHz band, On-body antennas, Indoor propagation.

1. INTRODUCTION
Ageing of the global population is unprecedented and the number of older people is expected to exceed the number of younger people for the first time by 2050. People aged over 60 constituted 8% of the global population in 1950, 10% in 2000 and is estimated to be 21% in 2050 [1]. The existing medical system will not be able to meet this increasing demand, and therefore the use of emerging digital technologies for healthcare monitoring is essential. Wireless Sensor Networks (WSNs), in particular, are expected to play an important role and many projects have already been developed in the area of body-centric wireless healthcare monitoring [2][3]. A comprehensive understanding of the wireless channel is important for any wireless communication system. The antennas and the radiowave propagation, which essentially constitute the basic elements of the channel, determine the quality and the reliability of the wireless link and hence have a great impact on the Quality-of-Service (QoS) offered by the whole system. In Wireless Body Area Networks (WBANs), in particular, the human body imposes a number of extra challenges such as electromagnetic absorption and propagation shadowing. The WBAN communications can be in general classified in four main categories:

1) In-body (communication inside the human body);
2) On-body (communication between two on-body nodes);
3) Body-to-body (communication between two on-body nodes mounted on two different bodies); and
4) Off-body (communication from an on-body node to a nearby access point (AP) located away from the body).

This paper focuses on the last category. A number of off-body channel measurements for Ultra-Wideband (UWB) applications (frequency range between 3.1 GHz to 10.6 GHz) have been presented in [4][5]. However, two of the main technologies that are currently widely used for body-centric wireless healthcare monitoring are Bluetooth Low Energy (BLE) and ZigBee [6][7]. They both operate over a narrow 2 MHz channel bandwidth at 2.4 GHz, while ZigBee also offers the option of the 868 MHz band (in Europe). There are only a limited number of publications that investigate the off-body wireless channel in the 2.4 GHz and the 868 MHz bands [8]-[10]. The objective of this paper is to present an off-body channel measurement campaign in an indoor laboratory environment in order to:

1) evaluate (and benchmark) the performance of different antennas in the 2.4 GHz band;
2) compare and quantify the advantages of propagation at 2.4 GHz and 868 MHz; and

3) develop a measurement-based channel model suitable for narrowband system-level simulations at 2.4 GHz.

The remaining of this paper is organised as follows:

Section 2 describes the measurement set-up, including a description of the antennas and the propagation environment (due to limited space only the 2.4 GHz antennas are analysed in detail). Section 3 presents the main results, which include a validation-of-concept measurement in the anechoic chamber, an antenna performance evaluation at 2.4 GHz, a comparison of propagation at 2.4 GHz and 868 MHz, and a channel model for narrowband system-level simulations at 2.4 GHz. Section 4 concludes the paper.

2. MEASUREMENT SET-UP

This section describes the set-up of the measurements. It should initially be stated that the measured parameter used in this paper is the off-body wireless channel gain. The main difference between channel gain and path-loss (PL) is that the former includes the transmit and receive antenna gains. The gain of an antenna is derived from its directivity taking into account the overall antenna efficiency [11]. The free-space path-loss, which occurs when no obstacles interrupt the wireless link, can theoretically be derived from equation 1 (in dB) [12]:

$$PL = 10log_{10}\left(\frac{4\pi d}{\lambda}\right)^2 \qquad (1)$$

where d is the separation distance between the transmitter and the receiver, and λ is the carrier wavelength. Although the channel gain was measured with the downlink in mind (i.e. the link from the AP transmitter to the on-body receiver), all results are reciprocal.
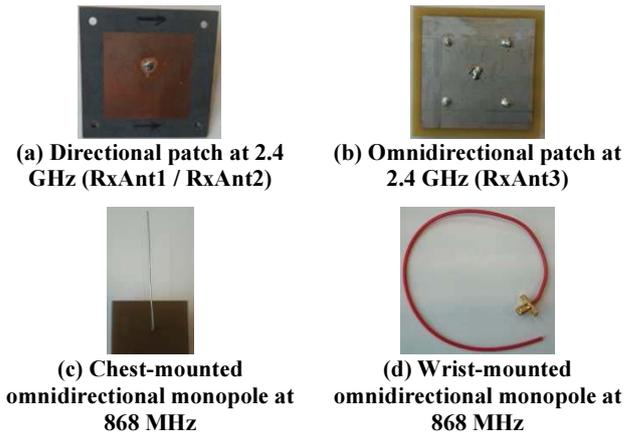
In both frequency bands, two orthogonal dipoles were used for the side of the AP (one vertical and one horizontal). Figure 1 presents the measured far-field radiation patterns of the 2.4 GHz AP antennas. All patterns are 3D, were measured in the anechoic chamber at 2440 MHz and are presented colour-coded according to directivity and polarisation. Table 1 summarises the pattern statistics. TxAnt1 (vertical dipole) radiates mainly in parallel to the floor (x-y plane), with 92% of the power in vertical polarisation and a maximum directivity of 4.7 dBi for the vertically polarised component of the pattern. TxAnt2 (horizontal dipole) radiates with 74% of the power concentrated in the horizontal polarised component of the pattern and a maximum directivity of 3.9 dBi and 5.2 dBi for the vertical and the horizontal polarisation component respectively. In this case, the antenna transmits most of its energy in a plane perpendicular to the floor (y-z plane). The efficiency of the antennas was also measured, following the method described in [13]. The measurement is relative to a highly-efficient monopole on a very large ground plane radiating at the same frequency as the antenna-under-test, includes all mismatch and dielectric/conduction losses, and showed an accuracy of ±5%. As expected, both dipoles proved to be very efficient, with a measured efficiency of 95%.

(a) TxAnt1 – Directivity   **(b) TxAnt1 – Polarisation**

(c) TxAnt2 – Directivity   **(d) TxAnt2 – Polarisation**
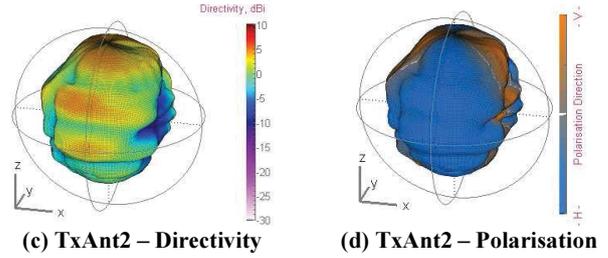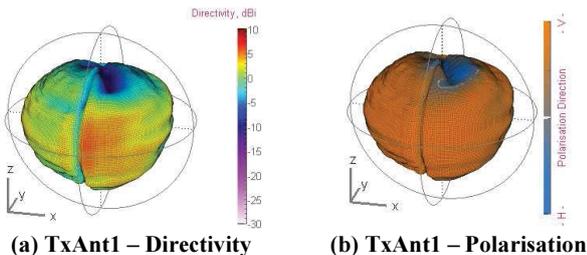
Figure 1. Measured far-field radiation patterns of AP antennas at 2440 MHz. V and H refer to the vertical and the horizontal polarisation component of the radiation pattern respectively.

Table 1. Measured antenna characteristics at 2440 MHz. V and H refer to the vertical and the horizontal polarisation component of the radiation pattern respectively.

	Max directivity (V) (dBi)	Max directivity (H) (dBi)	Power concentration (V) (%)	Power concentration (H) (%)	Efficiency (%)
TxAnt1	4.7	-4.0	92	8	95
TxAnt2	3.9	5.2	26	74	95
RxAnt1	-4.3	8.5	9	91	45
RxAnt2	8.5	0.3	94	6	45
RxAnt3	4.7	5.3	35	65	30

(a) Directional patch at 2.4 GHz (RxAnt1 / RxAnt2)   **(b) Omnidirectional patch at 2.4 GHz (RxAnt3)**

(c) Chest-mounted omnidirectional monopole at 868 MHz   **(d) Wrist-mounted omnidirectional monopole at 868 MHz**

Figure 2. On-body receiver antennas.

At the on-body receiver side, two different antennas were used in each frequency band and are shown in Figure 2. At 2.4 GHz, a directional patch antenna on RT/Duroid 5880 substrate [14] was used in two orthogonal polarisations, with RxAnt1 referring to the horizontally polarised element and RxAnt2 to its 90º rotation (vertically polarised element). The other 2.4 GHz receive antenna (RxAnt3) was a horizontally polarised omnidirectional patch on FR4 substrate, which produces a monopole-like radiation pattern [15]. It should be noted that all 2.4 GHz antennas were chest-mounted. In order to measure the antennas in the anechoic chamber as realistically as possible, and due to the lack of a human body phantom, the antennas were mounted on a plastic torso-shape phantom which was fully covered with the absorbing material Eccosorb (by Emerson and Cuming). This was performed in order to take into account the shadowing and the absorption of the human body. Figure 3 shows the measured far-field radiation patterns and Table 1 summarises the pattern statistics. It can be

seen that both directional patches radiate more than 90% of the power in the dominant polarisation component of the pattern (i.e. horizontal for RxAnt1 and vertical for RxAnt2) with a maximum directivity of 8.5 dBi and an efficiency of 45%. The direction of radiation is perpendicular to the surface of the patches with a maximum on a plane parallel to the floor (x-y plane). The omnidirectional patch (RxAnt3) has 65% of the power concentrated in the horizontal polarisation component with a maximum directivity of 4.7 dBi and 5.3 dBi for the vertical and the horizontal polarisation component respectively. The radiation is mainly parallel to the body (y-z plane) and the measured efficiency is 30%.

(a) RxAnt1 – Directivity

(b) RxAnt1 – Polarisation

(c) RxAnt2 – Directivity

(d) RxAnt2 – Polarisation

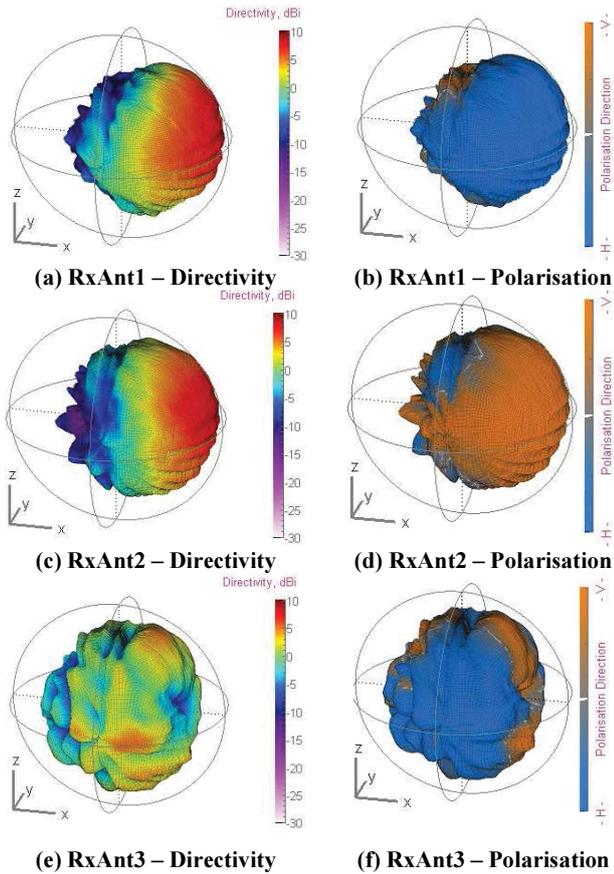**(e) RxAnt3 – Directivity**

(f) RxAnt3 – Polarisation

Figure 3. Measured far-field radiation patterns of on-body antennas at 2440 MHz. V and H refer to the vertical and the horizontal polarisation component of the radiation pattern respectively. Body positioned on the y-z plane.

Due to the larger physical size of the antennas at 868 MHz, patch antennas were not considered in this lower frequency band. A chest-mounted and a wrist-mounted omnidirectional monopole were used instead, both in two orthogonal polarisations. It should be noted that although very good matching was difficult to be achieved with the wrist-mounted monopole without a matching circuit (due to the lack of ground plane), the mismatch losses have been compensated for in the results that follow for a fair comparison.

All off-body channel gain measurements were performed using a human body subject (176 cm height; 78 kg weight) in an indoor laboratory environment. Figure 4 shows the plan of the laboratory and Figure 5 illustrates two indicative pictures. As it can be seen,

the subject was sitting on a stool, which was mounted on a turntable and rotated in azimuth through 360º with the help of motors. The location and the orientation of the AP transmitter remained fixed on a bench at a height of 90 cm from the floor, whereas four different user locations were considered at distances of 1.2 m, 2 m, 3.2 m and 4.5 m from the AP. 801 samples of the channel gain were recorded every 10º using a Vector Network Analyser (VNA) over a 100 MHz bandwidth in the 2.4 GHz band (2390 MHz to 2490 MHz) and a 0.6 MHz bandwidth in the 868 MHz band (868 MHz to 868.6 MHz). All measurements were performed twice (clockwise and anticlockwise rotation of the subject) and results have been averaged. Figure 6 shows an example of a channel measurement as a function of frequency and body azimuth rotation. The impact of the body shadowing and of the fast-fading is clear, as large channel gain variations can be noticed (up to about 40 dB difference between the maximum and the minimum recorded value in this example).
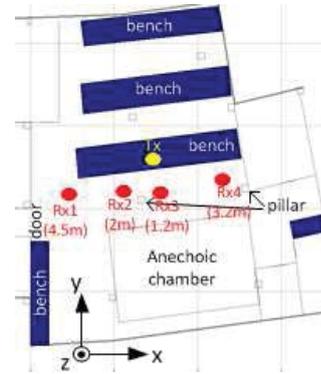
Figure 4. Plan of laboratory showing the AP transmitter (Tx) and the on-body receiver (Rx) locations.

Figure 5. Indicative pictures of the measurements showing the human body subject sitting on the stool in the laboratory environment.
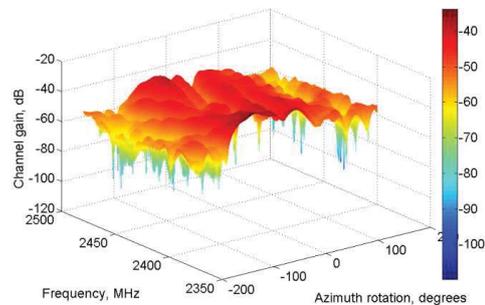
Figure 6. Example of channel gain measurement as a function of frequency and body azimuth rotation.

3. RESULTS

3.1 Validation-of-concept Measurements in Anechoic Chamber

In order to ensure the validity of our measurement procedure, a set of off-body channel gain measurements was initially conducted in the anechoic chamber in the 2.4 GHz band. The separation distance between the transmitter (AP) and the receiver (human subject) was set at 3.5 m. As in the indoor environment measurements, the human subject was rotated on the turntable through 360°, while the AP position and orientation remained constant. 801 samples of channel gain measurements were recorded using the VNA over a 100 MHz bandwidth (2390 MHz to 2490 MHz) every 10°.

Figure 7 shows the measured channel gain (averaged over the 100 MHz bandwidth) as a function of the body rotation for the co-polarisation (co-pol) component (i.e. vertical transmitter-to-vertical receiver or horizontal transmitter-to-horizontal receiver) of the three different on-body antennas. Furthermore, the maximum expected channel gain is also illustrated with a straight black line. This was theoretically calculated for the direct Line-of-Sight (LoS) path between the transmitter and the receiver using the maximum directivity and efficiency values reported in Table 1.

It can be noticed that in all cases the maximum measured channel gain lies within approximately 1 dB from the theoretical calculation. This ensures the validity of this measurement campaign. Figure 7 also highlights the impact of the human body shadowing. It can be seen that in an anechoic environment, an attenuation of about 30 dB and 20 dB is introduced by the body when directional and omnidirectional patch antennas are used respectively for the on-body (chest-mounted) node in the 2.4 GHz band. This constitutes a significant challenge for off-body wireless communications.
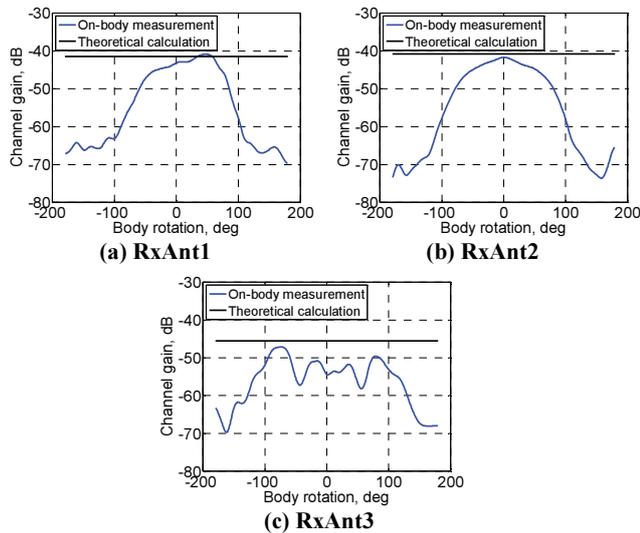

(a) RxAnt1

(b) RxAnt2

(c) RxAnt3

Figure 7. Validation-of-concept measurements in the anechoic chamber at 2.4 GHz (co-pol component).

3.2 Performance Evaluation of Different Antennas at 2.4 GHz

This sub-section compares and quantifies the performance of the different AP and on-body antenna combinations in the indoor laboratory environment in the 2.4 GHz band. Figure 8 shows the Cumulative Distribution Functions (CDFs) of the average (over the 100 MHz bandwidth) measured channel gain for the six transmit and receive antenna combinations. The CDFs have been computed over all receiver locations and body orientations.

It can be noticed that the on-body directional patch antennas, if they are aligned in polarisation with the AP antennas, result in an approximately 4 dB higher channel gain in average (i.e. for a CDF value of 50 in the vertical axis) than the omnidirectional ones. This is mainly due to the fact that the horizontally polarised omnidirectional antennas radiate most of the energy along and around the body rather than towards the room, as the directional antennas do (this can be seen in the radiation patterns of Figure 3). Hence, they would probably be better for on-body communications, while the directional patches should be preferred for off-body wireless links.

However, transmit and receive antenna polarisation misalignment for the directional patch antennas results in an average of about 6 dB lower channel gain. The omnidirectional patches, on the other hand, are less sensitive to polarisation misalignment, as in 90% of the cases the difference between the two polarisations lies within only about 0.5 dB.
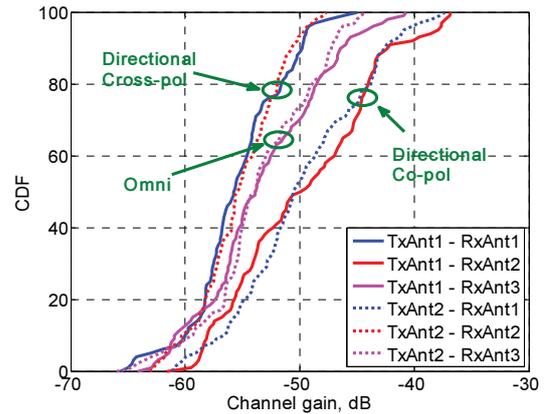

Figure 8. Comparison of CDFs (over all receiver locations and body orientations) of channel gain for different transmit (AP) and receive (on-body) antenna combinations at 2.4 GHz.

3.3 Comparison of Propagation at 2.4 GHz and 868 MHz

This sub-section compares the wireless propagation in the 2.4 GHz and the 868 MHz bands. According to equation 1, the free-space path-loss is inversely proportional to the carrier wavelength, and hence proportional to the frequency of operation. Using equation 1, it is expected that the channel gain at 868 MHz will be about 9 dB higher than at 2.4 GHz.

However, this calculation is valid only if the antennas have the same patterns and efficiencies in the two bands. Since the size of the antennas is also inversely related to the frequency, it can be understood that the antenna design at 868 MHz is more challenging. For example, the equivalent to a 40 mm square patch

on RT/Duroid 5880, which was used for the 2.4 GHz measurements of this paper, would require a dimension of approximately 115 mm for operation at 868 MHz. This large antenna size is prohibitive for on-body sensor nodes. On-body nodes require small antennas, and reducing the size of a large 868 MHz antenna will result in distortion of the pattern, low efficiency values and narrow bandwidth (with the latter not being necessarily a big problem as the 868 MHz band is quite narrow with a bandwidth of 0.6 MHz).

Figure 9 shows a comparison of the measured channel gain in the two bands (only the co-polarisation component of four indicative cases is shown here). The CDFs were computed over all receiver locations and body orientations in the laboratory environment. The straight lines refer to 2.4 GHz (reproduced from Figure 8 for a more convenient comparison) and the dotted lines to 868 MHz.

The first conclusion can be drawn if antennas with similar patterns in both bands are compared. It can be seen that using chest-mounted horizontally polarised omnidirectional antennas in both bands (i.e. straight pink and dotted black lines in Figure 9), the 868 MHz band results in an average of approximately 5 dB and a maximum of about 7 dB higher channel gain. It should be noted that this 2 dB lower than the theoretically expected maximum channel gain difference of 9 dB between the two bands is probably due to the different antennas used for the measurements.

However, if directional on-body patch antennas are used at 2.4 GHz (straight blue line in Figure 9) the benefit of the 868 MHz band is only about 1 dB in average. This underlines the advantage of the higher frequency band, which offers more flexibility in the antenna design and can thus compensate for the higher free-space path-loss.

It can also be noticed that the wrist-worn antenna results in about 6 dB lower channel gain than the chest-worn one at 868 MHz. This result agrees with the trend noticed in [10], where an average difference of about 10 dB was measured between a chest-worn and a wrist-worn antenna in an indoor environment (for distances from the AP between 1 m and 4 m and body rotation through 360º). Further investigation is required in order to identify the reasons behind this result (including the study of the behaviour of different antenna designs and in different frequency bands).
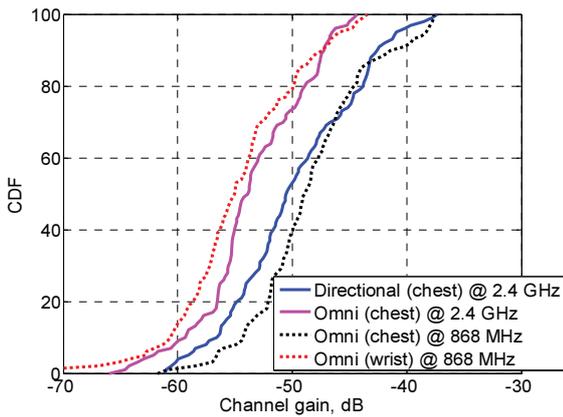
Figure 9. Comparison of CDFs (over all receiver locations and body orientations) of channel gain at 2.4 GHz and at 868 MHz (co-pol components).

3.4 Channel Model for Narrowband System-level Simulations at 2.4 GHz

This sub-section presents a measurement-based indoor channel model suitable for driving narrowband system-level simulators at 2.4 GHz. System-level simulations are essential in order to evaluate and eventually optimise the performance of a communication system. As it has already been mentioned, two of the most commonly used technologies for body-centric low-power wireless communications are the BLE and ZigBee, both of which operate over a narrow 2 MHz channel bandwidth at 2.4 GHz. It should be noted that the minimum resolution in time between two distinct multipath components that a system can resolve is inversely proportional to its bandwidth, in this case equal to 500 ns. The measurements, on the other hand, showed a maximum excess delay of about 150 ns (applying a 30 dB window to the power delay profile). This means that for systems such as BLE and ZigBee with narrow bandwidth the wireless channel should be modelled as a single tap.

The first step of the channel modelling procedure is to compute the average channel gain of the tap as a normal variable with mean and standard deviation from Table 2. The values of Table 2 are based on the measurements and are reported as a function of transmit and receive antenna pair, distance between the AP and the user (1.2, 2, 3.2 or 4.5 m), and user body orientation. As shown in Figure 10, the body rotation was divided in four 90º-wide sectors (anti-clockwise), with the reference of 0º referring to the direct LoS line between the user (human subject) and the AP.
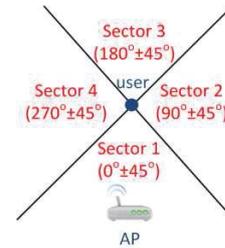
Figure 10. Orientation of the user with respect to the AP.

The next step is to add fast-fading. Fast-fading refers to the rapid variations of the channel gain for very small spatial or frequency changes due to the constructive or destructive vector summation of the multipath components [12]. In order to model the statistical distribution of fast-fading, the measured channel gain was sampled over the 100 MHz measurement bandwidth with a sampling rate equal to the coherence bandwidth. The latter was calculated as the frequency shift for which the auto-correlation coefficient of the channel frequency response falls below 0.5 for the first time. Sampling at a rate equal to the coherent bandwidth ensures that the sampled channel gain values are independent. This procedure was performed per transmit and receive antenna pair and per body rotation sector. The Probability Density Function (PDF) of the normalised (to the mean) channel gain was then computed and the best-fit distributions were found using the Anderson-Darling test [16]. A number of commonly used distributions (Rayleigh, Rician, Gamma, Normal, Lognormal, Weibull and Nakagami) were compared to the measurements, and as best-fit distribution was chosen the one that resulted in the lowest statistic value.

Table 2. Average (μ) and standard deviation (σ) of measured channel gain at 2.4 GHz in dB.

		1.2m		2m		3.2m		4.5m	
		μ	σ	μ	σ	μ	σ	μ	σ
TxAnt1 – RxAnt1	**Sector 1**	-50.5	0.7	-48.8	2.5	-50.5	1.6	-54.7	0.7
	Sector 2	-55.2	2.5	-54.5	2.2	-55.9	3.1	-58.4	1.3
	Sector 3	-57.2	1.2	-56.8	0.7	-58.7	1.4	-64.2	1.1
	Sector 4	-54.7	1.8	-54.5	2.9	-54.9	2.9	-58.1	1.5
TxAnt1 – RxAnt2	**Sector 1**	-37.5	0.5	-44.0	1.2	-44.6	1.0	-45.1	1.4
	Sector 2	-47.7	4.4	-44.9	2.9	-51.8	2.9	-50.7	4.4
	Sector 3	-53.3	1.6	-56.0	0.5	-57.6	1.6	-58.7	1.2
	Sector 4	-47.2	5.5	-50.1	4.8	-50.3	3.1	-55.2	3.7
TxAnt1 – RxAnt3	**Sector 1**	-42.8	1.4	-46.7	0.8	-52.7	1.5	-50.1	1.4
	Sector 2	-53.8	3.3	-47.9	1.4	-57.6	2.3	-52.4	3.2
	Sector 3	-56.1	1.0	-55.0	1.3	-61.5	1.4	-61.5	0.9
	Sector 4	-51.7	3.8	-51.7	3.6	-56.4	1.5	-55.5	2.3
TxAnt2 – RxAnt1	**Sector 1**	-39.4	1.4	-43.8	0.9	-44.1	2.2	-49.9	0.9
	Sector 2	-48.9	4.6	-44.5	1.9	-51.7	2.9	-52.1	3.8
	Sector 3	-52.1	0.8	-54.2	2.0	-54.5	1.5	-59.8	1.1
	Sector 4	-49.2	3.6	-47.6	3.7	-50.0	3.4	-55.1	3.5
TxAnt2 – RxAnt2	**Sector 1**	-49.3	1.3	-51.0	1.1	-51.6	1.2	-54.7	1.8
	Sector 2	-53.9	2.3	-53.4	2.2	-55.9	1.9	-57.5	2.7
	Sector 3	-55.5	1.1	-58.1	0.9	-56.7	1.0	-61.5	0.9
	Sector 4	-54.7	1.7	-55.8	2.6	-54.6	2.4	-59.8	2.2
TxAnt2 – RxAnt3	**Sector 1**	-47.9	2.0	-48.4	2.5	-48.2	1.3	-55.2	1.0
	Sector 2	-49.4	2.5	-50.3	3.6	-55.5	1.5	-56.9	2.4
	Sector 3	-55.1	1.2	-54.1	1.4	-56.8	2.0	-63.4	1.6
	Sector 4	-49.3	2.4	-53.7	1.9	-54.7	3.3	-58.0	2.2

Figure 11 shows an example of the PDF of the normalised envelope for the four body orientation sectors of the antenna pair TxAnt1 and RxAnt2. The best-fit distribution is also illustrated (red line). A narrow PDF with more values concentrated around unity indicates small channel variations, as is the case for Sector 1 where the communication is dominated by the direct LoS path between the transmit and the receive antennas. On the other hand, a wider PDF indicates more severe channel variations, as is the case for Sector 3 where the Non-LoS wireless link consists mainly of the reflected, diffracted and scattered multipath components. As expected, the distributions for Sectors 2 and 4, which represent the "body side-to-AP" cases, resulted in-between (i.e. wider than Sector 1 and narrower than Sector 3). Table 3 summarises the best-fit distributions for all transmit and receive antenna pairs and body orientations.

Finally, in order to obtain a statistically valid set of system-level performance results, the aforementioned procedure must be repeated until a large number of channel realisations are implemented for each link.

(c) Sector 3 **(d) Sector 4**
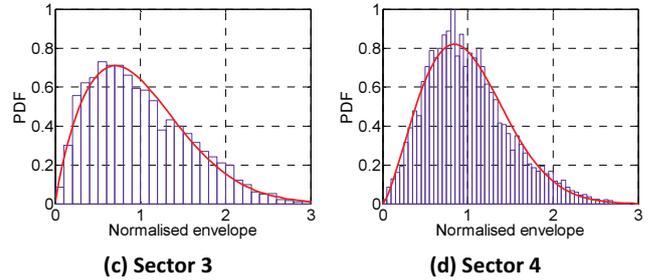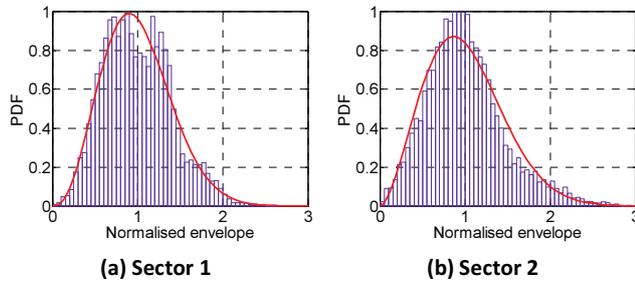
Figure 11: Example of PDF of normalised (to the mean) envelope and best-fit distributions (TxAnt1 – RxAnt2).

Table 3. Best-fit fast-fading distributions of the signal envelope (relative to the mean) at 2.4 GHz.

		Best-fit distribution
TxAnt1 – RxAnt1	**Sector 1**	**Gamma**, a=4.02 and b=0.24
	Sector 2	**Nakagami**, mu=1.09 and omega=1.25
	Sector 3	**Weibull**, A=1.13 and B=1.92
	Sector 4	**Gamma**, a=3.40 and b=0.29
TxAnt1 – RxAnt2	**Sector 1**	**Nakagami**, mu=1.65 and omega=1.15
	Sector 2	**Nakagami**, mu=1.30 and omega=1.20
	Sector 3	**Weibull**, A=1.12 and B=1.77
	Sector 4	**Nakagami**, mu=1.16 and omega=1.23
TxAnt1 – RxAnt3	**Sector 1**	**Rician**, s=0.86 and sigma=0.45
	Sector 2	**Weibull**, A=1.12 and B=2.22
	Sector 3	**Rician**, s=0.68 and sigma=0.62
	Sector 4	**Rician**, s=0.79 and sigma=0.54
TxAnt2 – RxAnt1	**Sector 1**	**Nakagami**, mu=1.36 and omega=1.18
	Sector 2	**Nakagami**, mu=1.12 and omega=1.23
	Sector 3	**Gamma**, a=3.38 and b=0.29
	Sector 4	**Nakagami**, mu=1.14 and omega=1.23

(a) Sector 1 **(b) Sector 2**

TxAnt2 – RxAnt2	**Sector 1**	**Rician**, s=0.67 and sigma=0.62
	Sector 2	**Weibull**, A=1.12 and B=1.92
	Sector 3	**Weibull**, A=1.12 and B=1.93
	Sector 4	**Gamma**, a=2.98 and b=0.33
TxAnt2 – RxAnt3	**Sector 1**	**Rician**, s=0.85 and sigma=0.46
	Sector 2	**Rician**, s=0.79 and sigma=0.54
	Sector 3	**Rician**, s=0.76 and sigma=0.56
	Sector 4	**Rician**, s=0.75 and sigma=0.57

4. CONCLUSIONS

This paper presented an off-body wireless channel measurement campaign in an indoor laboratory environment at 2.4 GHz and 868 MHz.

The performance of different antennas at 2.4 GHz was initially evaluated. It was shown that directional patch chest-mounted on-body antennas, when aligned in polarisation with the AP antennas, resulted in an average of 4 dB higher channel gain than the horizontally polarised omnidirectional ones. However, polarisation mismatch for the patches resulted in an average of 6 dB lower channel gain, while the omnidirectional antennas were within only 0.5 dB in 90% of the cases. The use of directional patches would hence be recommended for the on-body node provided polarisation alignment with the AP can be ensured. This could possibly be achieved by adding some intelligence such as polarisation diversity or antenna switching to the AP side.

Propagation was then compared between the 2.4 GHz and the 868 MHz frequency bands. It was shown that when chest-mounted horizontally polarised omnidirectional antennas were used in both bands, the 868 MHz resulted in an average of 5 dB higher channel gain. However, when directional patches were used in the 2.4 GHz band, the advantage of the lower frequency was only about 1 dB in average. This underlines the advantage of the 2.4 GHz frequency band, which offers more flexibility in the antenna design and can thus compensate for the higher path-loss.

It was also found that the wrist-worn antenna resulted in 6 dB lower channel gain than the chest-mounted one at 868 MHz. This result agrees with the trend noticed in other experimental studies reported in literature, but needs further investigation.

Finally, a measurement-based channel model was proposed. The model incorporates the measured average channel gain values and fast-fading distributions, and is suitable for narrowband system-level simulations, such as BLE and ZigBee.

5. ACKNOWLEDGMENTS

6. REFERENCES

[1] United Nations Department of Economic and Social Affairs Population Division, "World Population Ageing: 1950-2050" (executive summary), http://www.un.org/esa/population/publications/worldageing19502050/, accessed May 2014.

[2] A. Pantelopoulos and N.G. Bourbakis. "A Survey on Wearable Sensor-Based Systems for Health Monitoring and Prognosis." *IEEE Transactions on Systems, Man, and Cybernetics, Part C: Applications and Reviews*, no. 1, 2010.

[3] M. Chen, S. Gonzalez, A. Vasilakos, H. Cao, and V.C. Leung. "Body Area Networks: A Survey." *Mob. Netw. Appl.*, no. 2, pp. 171–193, April 2011.

[4] M.M. Khan, Q.H. Abbasi, A. Alomainy, Y. Hao, and C. Parini, "Experimental Characterisation of Ultra-wideband Off-body Radio Channels Considering Antenna Effects." *IET Microwaves, Antennas Propagation*, no. 5, pp. 370–380, 2013.

[5] A. Goulianos, T.W.C. Brown, B.G. Evans, and S. Stavrou. "Wideband Power Modeling and Time Dispersion Analysis for UWB Indoor Off-Body Communications." *IEEE Transactions on Antennas and Propagation*, no. 7, pp. 2162–2171, 2009.

[6] H. Cao, V. Leung, C. Chow, and H. Chan. "Enabling Technologies for Wireless Body Area Networks: A Survey and Outlook." *IEEE Communications Magazine*, no. 12 pp. 84–93, 2009.

[7] K. Mikhaylov, N. Plevritakis, and J. Tervonen. "Performance Analysis and Comparison of Bluetooth Low Energy with IEEE 802.15.4 and SimpliciTI." *Journal of Sensor and Actuator Networks*, no. 3, pp. 589–613, August 2013.

[8] S.L. Cotton and W.G. Scanlon. "Measurements, Modeling and Simulation of the Off-Body Radio Channel for the Implementation of Bodyworn Antenna Diversity at 868 MHz." *IEEE Transactions on Antennas and Propagation*, no. 12, pp. 3951–3961, 2009.

[9] R. Rosini and R. D'Errico. "Off-Body Channel Modelling at 2.45 GHz for Two Different Antennas," *6th European Conference on Antennas and Propagation (EUCAP)*, pp. 3378–3382, 2012.

[10] D. Miniutti, et. al., "Narrowband on body to off body channel characterization for ban," IEEE 802.15-08-0559-00-0006, August 2008.

[11] C.A. Balanis, Antenna theory: Analysis and design, 3rd ed., J. Wiley & Sons, 2005.

[12] B. Sklar, "Rayleigh fading channels in mobile digital communication systems .I. Characterization," *IEEE Communications Magazine,* vol. 35, no. 7, pp. 90-100, 1997.

[13] G.S Hilton and H.W.W. Hunt-Grubbe, "Simulation and practical analysis of a cavity-backed linear slot antenna for operation in the IEEE802.11a band," *European Conformal Antenna Workshop (EWAC07)*, Sep. 2007.

[14] E. Mellios, G.S. Hilton, and A.R. Nix, "Optimising radio coverage for wireless media servers," *6th Loughborough Antennas and Propagation Conference (LAPC),* pp. 233-236, 2010.

[15] S. Dumanli, S. Gormus, and I.J. Craddock. "Energy Efficient Body Area Networking Based on Off-the-Shelf Wireless Sensors." *8th International Conference on Body Area Networks (BODYNETS)*, 2013.

[16] M.A. Stephens, "EDF Statistics for Goodness of Fit and Some Comparisons," *Journal of the American Statistical Association*, vol. 69, pp. 730–737, 1974.